
Universiteit
Leiden
The Netherlands

15N MAS NMR studies of Cph1 phytochrome:chromophore dynamics and intramolecular signal transduction

Rohmer, T.M.A.; Strauss, H.W.; Hughes, J.; Groot, H.J.M. de; Gartner, J.; Schmieder, P.; Matysik, J.

Citation
Rohmer, T. M. A., Strauss, H. W., Hughes, J., Groot, H. J. M. de, Gartner, J., Schmieder, P., & Matysik, J. (2006). 15N MAS NMR studies of Cph1 phytochrome:chromophore dynamics and intramolecular signal transduction. *Journal Of Physical Chemistry B*, *110*(41), 20580-20585. doi:10.1021/jp062454+

Version:	Publisher's Version
License:	Licensed under Article 25fa Copyright Act/Law (Amendment Taverne)
Downloaded from:	https://hdl.handle.net/1887/3455648

Note: To cite this publication please use the final published version (if applicable).

^{15}N MAS NMR Studies of Cph1 Phytochrome: Chromophore Dynamics and Intramolecular Signal Transduction

Thierry Rohmer,[†] Holger Strauss,[‡] Jon Hughes,[§] Huub de Groot,[†] Wolfgang Gärtner,[||] Peter Schmieder,[‡] and Jörg Matysik*,[†]

Leiden Institute of Chemistry, Gorlaeus Laboratoria, Leiden University, P.O. Box 9502, 2300 RA Leiden, The Netherlands, Forschungsinstitut für Molekulare Pharmakologie, Robert-Rössle-Straβe 10, D-13125 Berlin, Germany, Pflanzenphysiologie, Justus-Liebig-Universität, Senckenbergstraβe 3, D-35390 Gieβen, Germany, and Max-Planck-Institut für Bioanorganische Chemie, Stiftstraβe 34−36, D-45470 Mülheim, Germany

Received: April 21, 2006; In Final Form: August 7, 2006

Solid-state nuclear magnetic resonance (NMR) is applied for the first time to the photoreceptor phytochrome. The two stable states, Pr and Pfr, of the 59-kDa N-terminal module of the cyanobacterial phytochrome Cph1 from *Synechocystis* sp. PCC 6803 containing a uniformly ^{15}N-labeled phycocyanobilin cofactor are explored by ^{15}N cross-polarization (CP) magic-angle spinning (MAS) NMR. As recently shown by ^{15}N solution-state NMR using chemical shifts [Strauss, H. M.; Hughes, J.; Schmieder, P. *Biochemistry* **2005**, *44*, 8244], all four nitrogens are protonated in both states. CP/MAS NMR provides two additional independent lines of evidence for the protonation of the nitrogens. Apparent loss of mobility during photoactivation, indicated by the decrease of line width, demonstrates strong tension of the entire chromophore in the Pfr state, which is in clear contrast to a more relaxed Pr state. The outer rings (A and D) of the chromophore are significantly affected by the phototransformation, as indicated by both change of chemical shift and line width. On the other hand, on the inner rings (B and C) only minor changes of chemical shifts are detected, providing evidence for a conserved environment during phototransformation. In a mechanical model, the phototransformation is understood in terms of rotations between the A−B and C−D methine bridges, allowing for intramolecular signal transduction to the protein surface by a unit composed of the central rings B and C and its tightly linked protein surroundings during the highly energetic Pfr state.

Downloaded via LEIDEN UNIV on September 7, 2022 at 14:26:03 (UTC).
See https://pubs.acs.org/sharingguidelines for options on how to legitimately share published articles.

I. Introduction

Phytochromes form a family of biliprotein photoreceptors first identified in higher plants[1] and more recently in prokaryotes and nonphotosynthetic bacteria (for reviews, see refs 2−5). The prosthetic chromophore is an open-chain tetrapyrrole, which is covalently bound via a thioether linkage to a cysteine generally in the N-terminal module of the apoprotein.[6,7] The chromophore used by plant phytochromes is phytochromobilin (PΦB, Figure 1A), while cyanobacterial phytochromes bind phycocyanobilin (PCB, Figure 1B). The photochemically active cyanobacterial phytochrome Cph1 and its truncated translation product Cph1Δ2 show physicochemical properties similar to plant phytochromes.[8−11] In the physiologically inactive and thermally stable state Pr, absorption of red light leads to a fast *Z/E* photoisomerization of the methine bridge between rings C and D.[12−14] This isomerization initiates a cascade of reactions involving geometrical changes of both chromophore and protein.[15−18] The product is the thermally stable, far-red absorbing state Pfr. Pr and Pfr are photochemically interconvertible. While photoconversion affects the kinase activity of the C-terminal catalytic domain,[11,19] the physiological significance of this and other light-induced changes is still unclear.

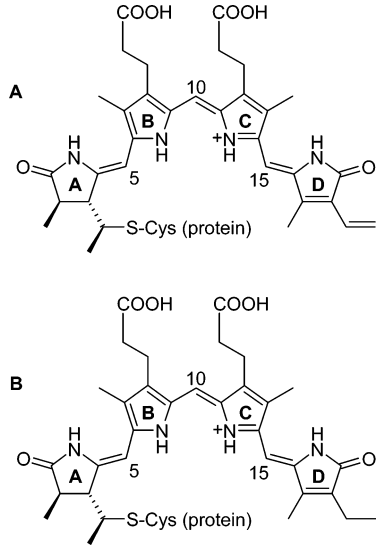

Figure 1. Structural formulas of PΦB (A) and PCB (B) shown in the *ZZZasa* geometry, as assumed for the Pr state.

Detailed knowledge of the structure and light-induced dynamics of the chromophore in its binding pocket is required to understand its photochemistry and the molecular rearrangements within the phytochrome protein. The protonation state of the nitrogen atoms of the chromophore throughout the photocycle has been a subject of debate.[20−22] Recently, it has been demonstrated by solution-state ^{15}N nuclear magnetic resonance

* To whom correspondence should be addressed. Phone: +31-71-527-4198; fax: +31-71-527-4603; e-mail: j.matysik@chem.leidenuniv.nl.
[†] Leiden University.
[‡] Forschungsinstitut für Molekulare Pharmakologie Berlin.
[§] Justus-Liebig-Universität Gieβen.
[||] Max-Planck-Institut Mülheim.

10.1021/jp062454+ CCC: $33.50 © 2006 American Chemical Society
Published on Web 09/23/2006

(NMR) experiments on the PCB chromophore in Cph1Δ2 that the chromophore is protonated in both Pr and Pfr states,[23] results we confirm and extend in the present paper using solid-state NMR methods.

Concerning the chromophore geometry, on the basis of vibrational spectroscopic studies,[17,18] Mroginski et al.[24] have provided convincing evidence that the photoconversion involves a *ZZZasa* (Pr) → *ZZEssa* (Pfr) geometry change. On the other hand, the recent 2.5 Å X-ray structure of the chromophore-bearing domain of BphP1 phytochrome from the bacterium *Deinococcus radiodurans* is more consistent with a *ZZZssa* configuration in the Pr state.[25] However, it should be borne in mind that such bacteriophytochromes carry a biliverdin IXα (instead of PCB or PΦB) cofactor bound to a different cysteine from that used by Cph1- and plant-type phytochromes and that the absorption properties of the Pfr state of this fragment are compromised, resulting in a bleached UV/vis spectrum (for discussion, see ref 6).

The exact mode of interaction between chromophore and protein is the subject of current research. In the Pr state, all four pyrrole rings appear to be tightly bound to the protein matrix by different interactions. Pyrrole ring A is covalently bound to cysteine C259 in Cph1,[6] while rings B and C are anchored by their propionate side chains extending deeply into the protein. The carbonyl group on ring D may form a hydrogen bond to a neighboring histidine, the vinyl group interacting hydrophobically with phenylalanines.[25]

Photoisomerization of the retinal chromophore in rhodopsin leads to loss of the chromophore and subtle conformational changes within the protein.[26] The photoactive yellow protein (PYP) has been shown to become unstable upon photoreaction around the *p*-coumaric acid chromophore and to start to unfold.[27,28] While the light-induced changes of the phytochrome have been discussed on the level of domain movement,[29,30] only little is known about those at the molecular level, although recent ultrafast absorbance measurements indicate a strong energetic coupling between chromophore and protein upon light activation (Müller et al., manuscript submitted for publication). It has been suggested that intermediate proton release and uptake by the chromophore may play a crucial role for the structural changes in the final step of the Pfr formation.[31] Pfr formation is associated with a large increase in mutual affinity of the sensory modules, perhaps providing a mechanism for molecular activation.[2,29,32] However, it is poorly understood how the photoisomerization of the PCB cofactor leads to large-scale structural changes of the entire complex.

High-resolution magic-angle spinning (MAS) NMR has evolved into a uniquely versatile tool for the elucidation of structure and dynamics in solid materials.[33,34] In the solid state, on one hand, anisotropic interactions as chemical shift anisotropy (CSA) and dipolar couplings broaden the signals, and on the other hand, they provide structural and dynamic information which is not present in the solution state. Hence, MAS NMR allows for investigation of dynamics of the chromophore in phytochrome and its change upon photoisomerization. To increase resolution, the magic-angle spinning technique mimics the averaging process present in solution without losing the desired directional information (for review, see ref 35). In conjunction with selective isotope labeling, MAS NMR allows for the study of cofactor properties down to the atomic level even in large protein complexes.[36]

In the present study, solid-state NMR has been applied to phytochrome for the first time. To investigate the light-triggered dynamics of the chromophore and its interaction with the protein pocket, by which the signal is transferred to the protein surface, we present ^{15}N cross-polarization (CP)/MAS NMR data of Cph1Δ2, containing a uniformly ^{15}N labeled PCB cofactor, in both the Pr and Pfr states.

II. Experimental Section

Cph1Δ2 as Model Compound for Plant Phytochrome. In the *Synechocystis* sp. PCC 6803 genome, a phytochrome gene, *slr0473*, encodes a 748-residue polypeptide. Heterologous expression in *Escherichia coli* yields an apoprotein that is capable of self-assembling with phycocyanobilin (PCB) to produce the photochemically active holophytochrome Cph1.[8,9,11] The truncated translation product Cph1Δ2, with a molecular weight of 59 kDa, comprises residues 1−514 plus a C-terminal His_6-tag. It binds covalently a PCB cofactor to form a red-/far-red photochromic holoprotein photochemically similar to full-length Cph1.[10]

Preparation of Labeled PCB. Axenic cultures of *Synechocystis* sp. PCC 6803 cells were cultivated at room temperature (24 ± 2 °C) in a modified BG11 medium in which $^{14}NO_3^-$ was replaced by $^{15}NO_3^-$.[23] Cells were grown in standard 2-L laboratory bottles under constant illumination with continuous white light (Sylvania Grolux, Osram, München, Germany). The cultures were constantly bubbled with air (6 L/min) provided by a standard laboratory pump fitted with a sterile filter (0.2 μm Acro 50, PALL, East Hills, United States) and were harvested when they reached stationary phase after ∼3−4 weeks (OD_{750} ∼ 2.5−3). All further manipulations of the cells used for the preparation of PCB were carried out at 18 °C to avoid disintegration of the phycobilisomes (PBS).[37] Cells were harvested by centrifugation at 5000*g* for 10 min, were resuspended in 30 mL of 0.75 M K_nPO_4 buffer (pH 7), and were broken with two passages through a French press at 120 MPa. The cellular debris was pelleted at 25 000*g* for 30 min. One milliliter of Triton X-100 was added to the supernatant which was shaken for 10 min; this solution was applied in aliquots of 5−6 mL to a discontinuous sucrose density gradient [7 mL of 0.5 M, 10 mL of 0.75 M, 7 mL of 1 M, and 7 mL of 1.5 M sucrose in 0.75 M K_nPO_4 buffer (pH 7)]. The mixture was put in 6 mm × 25 mm × 89 mm centrifuge tubes and was spun in the SW32 swing-out rotor for 18 h at 28 000 rpm in an LE 80K preparative ultracentrifuge (Beckman-Coulter, Palo Alto, United States). PBS (A_{622}/A_{280} > 3) accumulated in the 1 M sucrose layer. PBS were washed salt-free with distilled water in an Amicon pressure cell with a nominal molecular weight cutoff (NMWCO) of 10 kDa (Millipore, Bedford, United States). The PBS were lyophilized and subjected to methanolysis in a Soxhlett extractor for 24 h. These and subsequent steps were carried out in darkness or subdued light. PCB was concentrated to 2−10 mM with a rotary evaporator and was stored in methanol at −80 °C for no longer than 2 months before being used. The concentration of PCB was measured by absorption spectroscopy in a 5/95 (v/v) HCl/methanol mixture, using an E_{690} of 37.9 mM^{-1} cm^{-1}.[38]

^{15}N incorporation and the chemical identity of the isolated product were controlled with electrospray ionization mass spectroscopy and analytical HPLC using published procedures.[39] Both methods reveal a main fraction of correctly labeled PCB and negligible amounts of impurities. PCB prepared using this protocol yields the Cph1Δ2 holoprotein with spectral parameters in agreement with previously published data.[11]

Preparation of Cph1Δ2. Preparation of apo- and holoprotein was essentially performed as described previously.[40] Overnight culture of BL21-DE3 (Novagen) was grown in RB medium to

the early exponential phase ($OD_{600} \sim 0.4$) at 30 °C and was cooled on ice. BL21-DE3 cells additionally contained plasmid pSE111 encoding the *laqI*^{q} and *ArgU* genes. Expression was induced with 20 μM IPTG at 18 °C for 18 h, and then the cells were washed and concentrated in cold TES [50 mM Tris (pH 7.8), 5 mM EDTA, 300 mM NaCl] with 1 mM DTT added. Subsequent operations were carried out in darkness or under green safelight from 520-nm LEDs. Cells were lysed using two passages through the French press at 120 MPa. Before the first passage, ^{15}N labeled phycocyanobilin was added in darkness to the cell suspension. The crude extract was clarified at 25 000*g*, was precipitated with ammonium sulfate, was resuspended in 50 mM Tris (pH 7.8) and 300 mM NaCl, and was subjected to Ni^{2+}-affinity chromatography. Eluted holo-Cph1Δ2 was further purified by preparative size-exclusion chromatography in a Sephacryl S300 (Amersham Pharmacia/GE Healthcare) column in TES.

Sample Preparation for MAS NMR Spectroscopy. Samples for MAS NMR were concentrated using Vivaspin concentrators with an NMWCO of 30 kDa (Millipore). The solution was irradiated with far-red LEDs ($\lambda_{max} = 730$ nm, HHFW $\sim$ 30 nm) to reach almost 100% Pr. To generate a Pfr-saturated solution despite the absorbance of the solution in the red region of >30, samples were drawn into a 1 m long, 1 mm inner diameter glass capillary and were irradiated over the whole column with red LEDs ($\lambda_{max} = 660$ nm, HHFW $\sim$ 20 nm) until a photoequilibrium with ca. 70% of the sample in the Pfr state was reached. The photoequilibrium was checked by measuring the 500−800 nm spectrum of a small amount of sample, diluting it ~100-fold. The sample was then irradiated with far-red LED ($\lambda_{max} = 730$ nm) for 60 s to produce almost 100% Pr and a second spectrum was recorded as before. The efficiency of photoconversion was determined from the spectral difference at 655 and 708 nm.[9] This procedure resulted in a Pfr/Pr sample containing 70% Pfr and 30% Pr. For CP/MAS NMR experiments, the samples were then precipitated by addition of 3.3 M ammonium sulfate and were resuspended in 50 mM Tris (pH 7.8), 300 mM NaCl solution. The sample pellet of about 6 mg of protein was loaded into a 4-mm MAS rotor.

MAS NMR Measurement. The NMR experiments were performed using an AV-750 NMR spectrometer (Bruker GmbH, Karlsruhe, Germany) equipped with a dual-resonance MAS probe. The spectra were collected using cross-polarization and two-pulse phase modulation (TPPM) proton decoupling.[41] Spectra were obtained either at a rotational frequency $\omega_r/2\pi = 6$ kHz at a temperature of 223 K or at $\omega_r/2\pi = 8$ kHz at a temperature of 213 K. During initial freezing, the sample was spinning slowly (~600 Hz) to ensure a homogeneous sample distribution against the rotor wall.[42] Cycle delay was 2 s in all experiments. Each CP/MAS spectrum was recorded over a period of ca. 60 h. All ^{15}N chemical shifts were referenced to the response of solid glycine at 34.3 ppm.

III. Results

One-Dimensional $^{15}N_4$ CP/MAS NMR Spectra of [$^{15}N_4$] PCB−Cph1Δ2. The ^{15}N CP/MAS NMR spectra of Cph1Δ2 phytochrome containing uniformly [$^{15}N_4$] labeled PCB in both Pr and Pfr states are presented in Figure 2. The sharp signal at 24 ppm, visible in all spectra, derives from residual ammonium sulfate used for precipitation of the protein. The broad resonance at ~120 ppm is caused by the amide nitrogens of the protein backbone originating from ^{15}N-nitrogens in natural abundance. The spectrum of the Pr state (Figure 2A) shows three distinct maxima at 158, 147, and 132 ppm, while the spectrum of the Pfr/Pr mixture (Figure 2B) exhibits five maxima from the chromophore. Since the Pfr/Pr photoequilibrium mixture contains 70/30 Pfr/Pr, the maxima of Pfr have roughly twice the intensity of those attributed to Pr. The spectrum of the pure Pfr state has been obtained by subtraction using the maxima at 132 ppm as a marker of the Pr spectrum. The spectrum of pure Pfr (Figure 2C) shows three cofactor maxima at 158, 143, and 138 ppm. In neither spectrum do spinning sidebands occur. Spectra of the Pr state and of the Pfr/Pr mixture, recorded at 6 kHz and 223 K (data not shown), exhibit the same features as those presented in Figure 2.

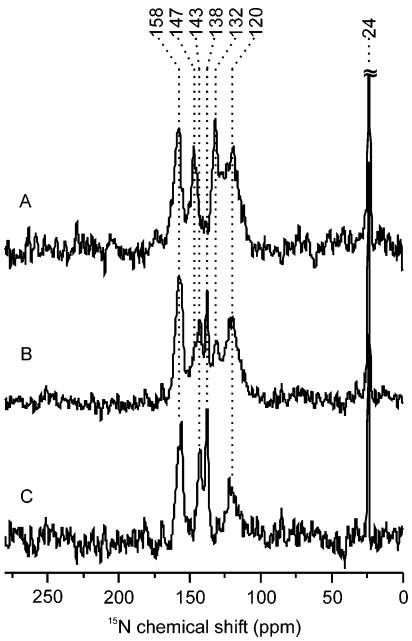

Figure 2. ^{15}N CP/MAS NMR spectra of [$^{15}N_4$] PCB−Cph1Δ2 in the Pr state (A) and a Pfr/Pr (70/30) photoequilibrium mixture (B) measured with a CP contact time of 2.048 ms, in a magnetic field of 17.2 T at 213 K. Each spectrum represents about 130 000 scans. The spinning frequency around the magic angle was 8.0 kHz. The spectrum of the pure Pfr state (C) has been obtained by subtraction.

Effect of the CP Contact Time. In the CP/MAS experiment, the nitrogens obtain magnetization by ^{1}H→^{15}N CP via Hartmann−Hahn matching. The effect of the CP contact time on the peak intensities and shapes of the chromophore signals in the Pr state has been investigated. To this end, spectra of the Pr state with contact times of 0.512, 2.048, and 4.096 ms were recorded (Figure 3). The shapes of the chromophore peaks appear to be independent of the contact time. The absolute intensity of the chromophore signal indicates an optimal CP contact time of 2.048 ms. The signals observed at 0.512 and 4.096 ms exhibit similar maximum of intensity, which are slightly lower than those at 2.048 ms. The identical behavior of all nitrogens suggests absence of mobile solvent molecules localized around one of these nitrogens. The backbone signal has the same intensities at 0.512 and 2.048 ms and decays slightly at 4.096 ms.

Lorentzian Deconvolution. In CP/MAS NMR, the signals are generally broader than those obtained by solution-state NMR. Lorentzian deconvolution of the Pr and pure Pfr spectra was thus applied to resolve overlapping signals and to obtain the accurate chemical shifts (Figure 4). The asterisks indicate the position of protein backbone signals in natural abundance. The chemical shifts of the simulated chromophore peaks have been determined at (i) 158.5, 146.8, and 132.1 ppm (1.9:1.0:1.1) for Pr (Figure 4A) and (ii) 156.9, 142.8, and 137.8 ppm (2.0:1.0:

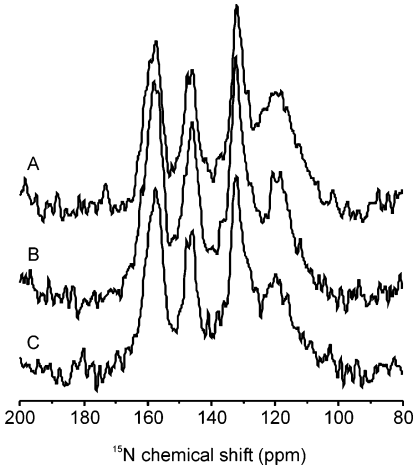

Figure 3. ^{15}N CP/MAS NMR spectra of [$^{15}N_4$] PCB−Cph1Δ2 in the Pr state measured with a CP contact time of 0.512 (A), 2.048 (B), and 4.096 ms (C) in a magnetic field of 17.2 T at 183 K. Each spectrum represents about 130 000 scans. The spinning frequency around the magic angle was 6.0 kHz.

1.0) for pure Pfr (Figure 4B) (Table 1). In the Pr state, the isolated peaks at 146.8 and 132.1 ppm show a half-height full width (HHFW) of 4.5 and 4.2 ppm, respectively. In the Pfr state, both isolated peaks are significantly narrowed, showing an HHFW of 3.3 ppm (142.8) and 2.2 ppm (137.8).

Intensity Ratio of the Nitrogen Signals in the Pr and Pfr States. In the Pr spectrum, the peak at lowest field (158.5 ppm) is broad and suitably fitted with a single peak, which has roughly twice the area of each of the isolated peaks (1.9:1.0:1.1). The spectrum of the Pfr state exhibits also a slightly shifted peak at 156.9 ppm, which also is fitted with one peak, and the ratio of the peak areas is 2.0:1.0:1.0. Therefore, in both spectra, the maxima at lowest field arise from two nitrogens. In addition, two well-separated chromophore peaks appear at 146.8/132.1 (Pr) and 142.8/137.8 ppm (Pfr), each of which corresponds to a single nitrogen. The slight difference in the peak area may originate from different CP efficiencies. The response of the protein backbone arises from all amino acids of the polypeptide in natural abundance. Within the present noise level, in both the Pr and Pfr spectra, the backbone resonances can be fit with a single Lorentzian peak. Thus, with the exception of the coalescence of two signals in the Pr and Pfr spectra, all four nitrogens have been unambiguously resolved in both phytochrome states.

IV. Discussion

Protonation State of the PCB Cofactor in the Pr and Pfr States. In both the Pr and Pfr states, the chemical shifts of all cofactor signals are below 160 ppm. In the past, solution state as well as CP/MAS NMR studies have shown that ^{15}N of deprotonated tetrapyrrole systems exhibit chemical shifts above 220 ppm, while those of protonated nitrogens are shifted at least 60 ppm upfield.[43,44] This is in line with the chemical shifts observed for protonated and deprotonated nitrogens in histidine by MAS NMR.[45,46] Hence, the observed chemical shifts provide clear evidence that all nitrogens of the chromophore are protonated in both Pr and Pfr states. Thus, the chromophore is positively charged in both Pr and Pfr states. This observation is in agreement with recent observations by solution-state NMR[23] demonstrating that the precipitation does not affect the state of the chromophore. In MAS NMR spectra, the chemical shift anisotropy (CSA) deduced from spinning sidebands provides additional information on the local electronic and protonic structure. Since the CSA is related to the symmetry of the ground-state electron density distribution around an atom, strong spinning sidebands indicate a large asymmetry of the local electronic structure. It has been shown that deprotonated nitrogens in histidine have a CSA that is much larger than protonated ones.[45,46] Therefore, the absence of rotational sidebands at rotational frequencies of 6 kHz (data not shown) and 8 kHz is well in line with protonated nitrogens, while from neutral nitrogens, with a local electronic structure deformed by the lone pair, an intense sideband pattern would be expected.

The CP/MAS NMR provides a third line of evidence on the protonation state of the chromophore nitrogens on the basis of the build-up kinetics of the ^{1}H→^{15}N CP transfer (for review, see ref 47). As shown in Figure 3, the ratio of all chromophore signals is independent of the CP contact time. This implies that all nitrogens have the same type of interaction with protons, and hence all nitrogens are protonated. The same conclusion can be made from the signal strength at contact times as short as 0.512 ms. The small intensity difference for signals obtained at 0.512 and the maximum at 2.048 ms is characteristic for directly protonated nitrogens, while hydrogen-bound nitrogens with a weaker hydrogen−nitrogen interaction are expected to be significantly less intense at short CP contact times. Therefore, we conclude that each nitrogen is protonated and that the nitrogens of the B and C rings do not share a common proton.

Signal Assignment. It has been established that all nitrogens of the cofactor are protonated and that the tetrapyrrole is positively charged. It is generally believed that the resulting positive charge is delocalized preferentially over rings B and C, and hence the nitrogen resonances of these rings are expected to shift to lower fields. In the case of the histidine residues in the light-harvesting complex II of *Rhodopseudomonas acidophila*, it has been shown that the protonated nitrogen of a cationic imidazole ring is roughly 8−10 ppm shifted downfield compared to the protonated nitrogen of a neutral imidazole.[45] This is in line with our assignment of nitrogens of rings B and C to the downfield-shifted signals at about 158 ppm. In addition, since the chemical structure of rings B and C is identical, similar chemical shifts are expected. Therefore, we assign the peak at 158.5 ppm in the Pr state and at 156.9 ppm in the Pfr state to both rings B and C. The two resolved signals of the spectra in both Pr and Pfr states can be attributed to the ^{15}N response from the nitrogens of rings A and D. Such an assignment implies that the Pr→Pfr photoisomerization affects mainly rings A and D, while rings B and C show little effect. In fact, Mroginski et al.[24] have shown that the double-bond isomerization at the C-15 methine bridge is likely to be followed by at least a partial single-bond rotation at the C-5 methine. In this way, converging evidence is obtained that the unit of rings B and C retains its structure and interactions with the protein upon photoisomerization.

During the Pr→Pfr photoisomerization, the ^{15}N chemical shift range is reduced. In the Pr state, the chemical shifts of the chromophore peaks are distributed over 26.4 ppm between 158.5 and 132.1 ppm, while in the Pfr state a range of 19.1 ppm from 156.9 to 137.8 ppm is observed. This result suggests an increase of the delocalization of the positive charge in the Pfr state.

Mobility of the PCB Cofactor. The Pr→Pfr transformation is accompanied by a remarkable reduction of the HHFW of all chromophore peaks. In both Pr and Pfr states, the maximum around 158 ppm was fitted by a single Lorentzian function. The reduction of the dynamics in the Pfr state leads to a narrowing of the maxima at lowest field (6.4 and 4.5 in the Pr and Pfr

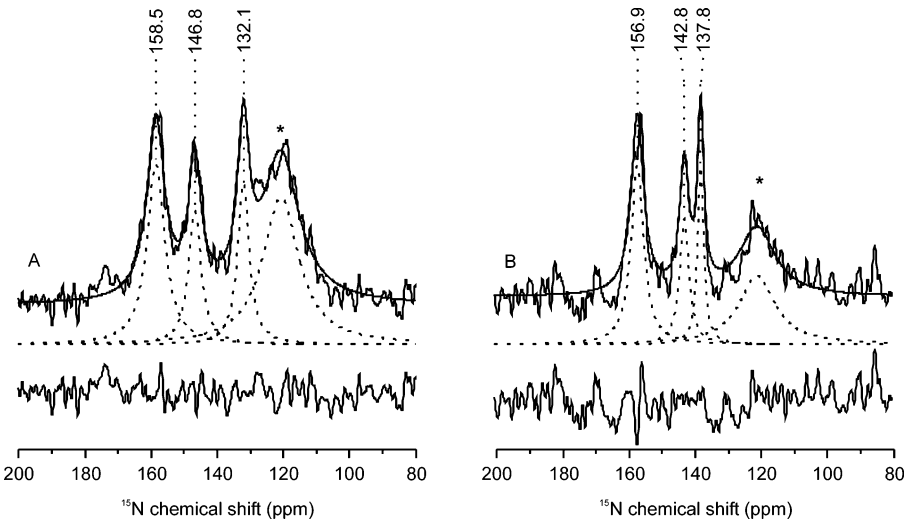

Figure 4. Lorentzian deconvolution of the ^{15}N CP/MAS NMR spectra of [$^{15}N_4$] PCB−Cph1Δ2 in the Pr (A) and Pfr (B) states. The upper part compares the experimental NMR spectrum with the sum of the Lorentzian fits. The lower part gives the individual Lorentzian fits (dashed line) and the residual spectra.

TABLE 1: Tentative Assignment of ^{15}N CP/MAS NMR Signals of [$^{15}N_4$] PCB−Cph1Δ2 in the Pr and Pfr States

Pr				Pfr			
δ_N (ppm)	HHFW (ppm)	relative area[a]	assignment	δ_N (ppm)	HHFW (ppm)	relative area[a]	assignment
158.5	(6.4)	1.9	B, C	156.9	(4.5)	2.0	B, C
146.8	4.5	1.0	A, D	142.8	3.3	1.0	A, D
132.1	4.2	1.1		137.8	2.2	1.0	

[a] Weakest signal set to unit.

state, respectively) (Table 1). In addition, the signals attributed to rings A and D also indicate a reduced dynamics at those positions. The reduced line width can result from reduced mobility of the chromophore. On the other hand, we cannot completely rule out an effect from solvent molecules in the binding pocket, however, the minor effect of the CP contact time on the signal strength as well as the same CP behavior of all four nitrogens suggests absence of mobile solvent molecules around one of these nitrogens. Therefore, the line narrowing during the Pr→Pfr transition originates most likely from a change of the chromophore mobility. The rigidity observed in Pfr may be related to the strong torsion of the C-15 methine bridge observed by Raman spectroscopy in the Pfr state.[17] Taking the reduction of the MAS NMR line width and the increased intensity of the Raman out-of-plane modes together, we would conclude that the chromophore in the Pfr state is tightly fixed, accompanied by a strong tension around the C-15 methine bridge. Hence, we tentatively assign the very narrow peak at 137.8 ppm in the Pfr spectrum to the nitrogen of ring D and thus the peak at 142.8 ppm to the nitrogen of ring A. If we assume that the peak at 137.8 ppm in the Pfr spectrum corresponds to the peak at 132.1 ppm in the Pr spectrum, the shift caused by the Pr→Pfr transformation would be 5.7 ppm compared to 4.0 ppm for the peak assigned to ring A. Such assignment would in fact match the expectation that the larger shift is observed at ring D, where the primary photochemistry occurs. Hence, photoisomerization at the C-15 methine bridge is linked to a loss of mobility of the entire chromophore in the Pfr state.

Model for Intramolecular Signal Transduction. The CP/MAS NMR data provide converging evidence that the inner rings B and C are only marginally affected by the Pr→Pfr photoconversion, while the outer rings A and D show significant effects on both chemical shifts and line widths. The invariance of the chemical shifts of the inner rings demonstrates that the protein environment remains mainly unchanged, especially because there is no significant change in counterionic interactions. Since the inner rings are tightly anchored to the protein by their propionate side chains,[25] we expect that they move together with their local protein environment without changing the chemical shifts of the pyrrole nitrogens. On the other hand, there is evidence that also rings A and D are fixed to the protein, for example, by covalent bonding of ring A to cysteine C259[6] and by interaction of ring D to the phenol ring of a neighboring tyrosine, which has been demonstrated to be crucial.[48] Hence, the concerted movement of the inner rings and their environment within the frame given by rings A and D and their protein environments must be linked to conformational changes in the protein structure. Such protein rearrangement can be related to the signal transduction to the surface. Such a mechanical model symbolized as A−(BC)−D implies fixation of the chromophore at both ends (A and D), two hinges (A−B and C−D), and a moving inner unit (rings B and C together with their protein surroundings) (Figure 5). This model could explain that the following conformational change occurs at the A−B hinge as proposed by Mroginski et al.,[24] while previous models expected an effect at the C-10 single bond.[17] As suggested by the change of dynamics upon photoisomerization, the chromophore can be considered as a spring, providing the force of moving the protein. In the Pr state, the mobility is high as in a relaxed spring, while in the Pfr state the stressed chromophore may retain the

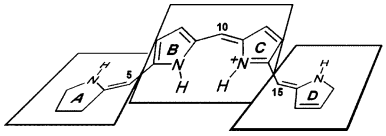

Figure 5. Mechanical model for signal transduction. The chromophore, symbolized as A−(BC)−D, is fixed at both ends (rings A and D), while a moving inner unit (rings B and C together with their surroundings) kept by two hinges (A−B and C−D), transfers the signal to the surface.

moving protein components. This proposal of a high-energy level of the Pfr state is also in line with mutation studies in which the formation of the Pfr state is impaired only allowing generation up to an intermediate state.[6] Furthermore, such interpretation is supported by several optical measurements showing that already the earliest intermediate of the Pfr→Pr back-conversion shows features of the Pr state[17,20] (Müller et al., manuscript submitted for publication).

V. Conclusions

From the ^{15}N CP/MAS NMR data of both Pr and Pfr stable states, it has been deduced that Pr→Pfr photoconversion is linked to a striking reduction of the chromophore mobility in the Pfr state. Upon photoconversion, the chemical shifts of peaks assigned to the inner rings B and C are weakly affected, while those of rings A and D show significant changes of chemical shifts. Hence, in our mechanical model for intramolecular signal transduction, the inner part of the chromophore (rings B and C as well as their tightly linked protein surroundings) transfers the light-induced signal to the protein surface, while rings A and D, which are also linked to the protein, provide the mechanical bearing for this rotation of the central unit. In this model, the chromophore behaves as a spring, relaxed in the Pr state and tensed in the Pfr state, allowing to move the protein to transfer the signal through the protein.

Acknowledgment. This paper is dedicated to Professor Kurt Schaffner on the occasion of his 75th birthday. Dr. Alia, Dr. S. Prakash, C. Erkelens, F. Lefeber, and J. Hollander are gratefully acknowledged for support during various stages of the experiments. T. R. and J. M. thank Dr. G. V. Kozhukh for his contribution and stimulating discussions. This work has been financially supported by the Volkswagen-Stiftung (I/79979) as well as by The Netherlands Organization for Scientific Research (NWO) by a Vidi award to J.M. (700.53.423).

Abbreviations

CP	cross-polarization
Cph1	cyanobacterial phytochrome 1
Cph1Δ2	N-ternimal, photochromic module of Cph1
CSA	chemical shift anisotropy
DTT	dithothreitol
HHFW	half-height full width
MAS	magic-angle spinning
NMWCO	nominal molecular weight cutoff
PBS	phycobilisome
PCB	phycocyanobilin
Pfr and Pr	far-red- and red-absorbing state of phytochrome, respectively
PΦB	phytochromobilin
sp.	species
TES	50 mM Tris (pH 7.8), 5 mM EDTA, 300 mM NaCl solution
TPPM	two-pulse phase modulation

References and Notes

(1) Butler, W. L.; Norris, K. H.; Siegelman, H. W.; Hendricks, S. B. *Proc. Natl. Acad. Sci. U.S.A.* **1959**, *45*, 1703.
(2) Hughes, J.; Lamparter, T. *Plant Physiol.* **1999**, *121*, 1059.
(3) Kim, J. I.; Kozhukh, G. V.; Song, P. S. *Biochem. Biophys. Res. Commun.* **2002**, *298*, 457.
(4) Montgomery, B. L.; Lagarias, J. C. *Trends. Plant. Sci.* **2002**, *7*, 357.
(5) Rockwell, N. C.; Su, Y. S.; Lagarias, J. C. *Annu. Rev. Plant. Biol.* **2006**, *57*, 837.
(6) Hahn, J.; Strauss, H. M.; Landgraf, F.; Faus Gimenèz, H.; Lochnit, G.; Schmieder, P.; Hughes, J. *FEBS J.* **2006**, *273*, 1415.
(7) Lagarias, J. C.; Rapoport, H. *J. Am. Chem. Soc.* **1980**, *102*, 4821.
(8) Hughes, J.; Lamparter, T.; Mittmann, F.; Hartmann, E.; Gärtner, W.; Wilde, A.; Börner, T. *Nature* **1997**, *386*, 663.
(9) Lamparter, T.; Mittmann, F.; Gärtner, W.; Börner, T.; Hartmann, E.; Hughes, J. *Proc. Natl. Acad.* Sci. *U.S.A.* **1997**, *94*, 11792.
(10) Sineshchekov, V.; Koppel, L.; Esteban, B.; Hughes, J.; Lamparter, T. *J. Photochem. Photobiol., B* **2002**, *67*, 39.
(11) Yeh, K. C.; Wu, S. H.; Murphy, J. T.; Lagarias, J. C. *Science* **1997**, *277*, 1505.
(12) Fodor, S. P. A.; Lagarias, J. C.; Mathies, R. A. *Biochemistry* **1990**, *29*, 11141.
(13) Kandori, H.; Yoshihara, K.; Tokutomi, S. *J. Am. Chem. Soc.* **1992**, *114*, 10958.
(14) Rüdiger, W.; Thümmler, F.; Cmiel, E.; Schneider, S. *Proc. Natl. Acad. Sci. U.S.A.* **1983**, *80*, 6244.
(15) Foerstendorf, H.; Mummert, E.; Schäfer, E.; Scheer, H.; Siebert, F. *Biochemistry* **1996**, *35*, 10793.
(16) Kneip, C.; Parbel, A.; Foerstendorf, H.; Scheer, H.; Siebert, F.; Hildebrandt, P. *J. Raman. Spectrosc.* **1998**, *29*, 939.
(17) Matysik, J.; Hildebrandt, P.; Schlamann, W.; Braslavsky, S. E.; Schaffner, K. *Biochemistry* **1995**, *34*, 10497.
(18) Remberg, A.; Lindner, I.; Lamparter, T.; Hughes, J.; Kneip, C.; Hildebrandt, P.; Braslavsky, S. E.; Gärtner, W.; Schaffner, K. *Biochemistry* **1997**, *36*, 13389.
(19) Yeh, K. C.; Lagarias, J. C. *Proc. Natl. Acad. Sci. U.S.A.* **1998**, *95*, 13976.
(20) Foerstendorf, H.; Benda, C.; Gärtner, W.; Storf, M.; Scheer, H.; Siebert, F. *Biochemistry* **2001**, *40*, 14952.
(21) Kneip, C.; Hildebrandt, P.; Schlamann, W.; Braslavsky, S. E.; Mark, F.; Schaffner, K. *Biochemistry* **1999**, *38*, 15185.
(22) Mizutani, Y.; Tokutomi, S.; Aoyagi, K.; Horitsu, K.; Kitagawa, T. *Biochemistry* **1991**, *30*, 10693.
(23) Strauss, H. M.; Hughes, J.; Schmieder, P. *Biochemistry* **2005**, *44*, 8244.
(24) Mroginski, M. A.; Murgida, D. H.; von Stetten, D.; Kneip, C.; Mark, F.; Hildebrandt, P. *J. Am. Chem. Soc.* **2004**, *126*, 16734.
(25) Wagner, J. R.; Brunzelle, J. S.; Forest, K. T.; Vierstra, R. D. *Nature* **2005**, *438*, 325.
(26) Spooner, P. J. R.; Sharples, J. M.; Goodall, S. C.; Bovee-Geurts, P. H. M.; Verhoeven, M. A.; Lugtenburg, J.; Pistorius, A. M. A.; de Grip, W. J.; Watts, A. *J. Mol. Biol.* **2004**, *343*, 719.
(27) Groenhof, G.; Bouxin-Cademartory, M.; Hess, B.; de Visser, S. P.; Berendsen, H. J. C.; Olivucci, M.; Mark, A. E.; Robb, M. A. *J. Am. Chem. Soc.* **2004**, *126*, 4228.
(28) Groenhof, G.; Lensink, M. F.; Berendsen, H. J. C.; Snijders, J. G.; Mark, A. E. *Proteins* **2002**, *48*, 202.
(29) Esteban, B.; Carrascal, M.; Abian, J.; Lamparter, T. *Biochemistry* **2005**, *44*, 450.
(30) Song, P. S. *J. Biochem. Mol. Biol.* **1999**, *32*, 215.
(31) Borucki, B.; von Stetten, D.; Seibeck, S.; Lamparter, T.; Michael, N.; Mroginski, M. A.; Otto, H.; Murgida, D. H.; Heyn, M. P.; Hildebrandt, P. *J. Biol. Chem.* **2005**, *280*, 34358.
(32) Strauss, H. M.; Schmieder, P.; Hughes, J. *FEBS Lett.* **2005**, *579*, 3970.
(33) Brown, S. P.; Spiess, H. W. *Chem. Rev.* **2001**, *101*, 4125.
(34) Wind, M.; Saalwächter, K.; Wiesler, U. M.; Müllen, K.; Spiess, H. W. *Macromolecules* **2002**, *35*, 10071.
(35) Laws, D. D.; Bitter, H. M. L.; Jerschow, A. *Angew. Chem., Int. Ed.* **2002**, *41*, 3096.
(36) de Groot, H. J. M. *Curr. Opin. Struct. Biol.* **2000**, *10*, 593.
(37) Glazer, A. N. *Methods Enzymol.* **1988**, *167*, 291.
(38) Chapman, D. J.; Cole, W. J.; Siegelman, H. W. *J. Am. Chem. Soc.* **1967**, *89*, 5976.
(39) Lindner, I.; Braslavsky, S. E.; Schaffner, K.; Gärtner, W. *Angew. Chem., Int. Ed.* **2000**, *39*, 3269.
(40) Lamparter, T.; Esteban, B.; Hughes, J. *Eur. J. Biochem.* **2001**, *268*, 4720.
(41) Bennett, A. E.; Rienstra, C. M.; Auger, M.; Lakshmi, K. V.; Griffin, R. G. *J. Chem. Phys.* **1995**, *103*, 6951.
(42) Fischer, M. R.; de Groot, H. J. M.; Raap, J.; Winkel, C.; Hoff, A. J.; Lugtenburg, J. *Biochemistry* **1992**, *31*, 11038.
(43) Falk, H.; Müller, N. *Magn. Reson. Chem.* **1985**, *23*, 353.
(44) Limbach, H. H.; Hennig, J.; Kendrick, R.; Yannoni, C. S. *J. Am. Chem. Soc.* **1984**, *106*, 4059.
(45) Alia; Matysik, J.; Soede-Huijbregts, C.; Baldus, M.; Raap, J.; Lugtenburg, J.; Gast, P.; van Gorkom, H. J.; Hoff, A. J.; de Groot, H. J. M. *J. Am. Chem. Soc.* **2001**, *123*, 4803.
(46) Wei, Y. F.; de Dios, A. C.; McDermott, A. E. *J. Am. Chem. Soc.* **1999**, *121*, 10389.
(47) Kolodziejski, W.; Klinowski, J. *Chem. Rev.* **2002**, *102*, 613.
(48) Fischer, A. J.; Lagarias, J. C. *Proc. Natl. Acad. Sci. U.S.A.* **2004**, *101*, 17334.